ELSEVIER

Palaeogeography, Palaeoclimatology, Palaeoecology 154 (1999) 237–246

PALAEO

Astronomical calibration of loess–paleosol deposits at Luochuan, central Chinese Loess Plateau

Huayu Lu [a,*], Xiaodong Liu [a,b], Fuqing Zhang [c], Zhisheng An [a], John Dodson [d]

[a] *State Key Laboratory of Loess and Quaternary Geology, Chinese Academy of Sciences, No. 22-2, Xiying road, Xi'an 710054, China*
[b] *Lanzhou Institute of Plateau Atmospheric Sciences, Chinese Academy of Sciences, Lanzhou 730000, China*
[c] *Department of Marine, Earth and Atmospheric Sciences, North Carolina State University, Raleigh, NC 27695-8208, USA*
[d] *Department of Geography, University of Western Australia, Perth, WA 6907, Australia*

Received 27 January 1998; accepted 8 June 1999

Abstract

The 140 m loess–paleosol profile at Luochuan in the central Chinese Loess Plateau was sampled at 5-cm intervals in loess units and at 3 cm in paleosol units, in order to obtain a high resolution climatic record covering the past 2.5 million years. All samples were measured for magnetic susceptibility, which is regarded as a good proxy index of the East Asian summer monsoon strength. On the basis of the astronomical theory of Pleistocene climatic change, an age model of the Luochuan loess–paleosol sequence was developed by tuning the magnetic susceptibility record to time-series of insolation changes. The results show that the ages of the boundaries between the Malan and Lishi, and Lishi and Wucheng loess formations are 71 and 1320 kyr BP, respectively. The onset of loess accumulation is at 2470 kyr BP. Our age model was tested by comparing the orbitally derived ages with absolute age determinations of magnetic reversals, and cross-spectrum analyzing with solar radiation variations for summer at 65ºN. These indicate that the calibration provides a reliable time scale for the Luochuan loess–paleosol deposit.

Keywords: loess deposits; time scale; orbital tuning; central Chinese Loess Plateau

1. Introduction

Several loess–paleosol deposits on the central Chinese Loess Plateau are regarded as continuous and complete continental records of Quaternary paleoclimate variations in North China (Liu et al., 1985; An et al., 1990; Ding et al., 1994). The age frame for the loess–paleosol sequence at Luochuan (Fig. 1) has been constructed by various authors (Heller and Liu, 1982; Liu et al., 1985; Kukla and An, 1989; Yue, 1995). The time scale published by Liu et al. (1985) was obtained by interpolating the sedimentation rate between the paleomagnetic reversal points, and it probably over-generalizes since it assumes that the rate of deposition was similar through all loess and paleosol units. The magnetic susceptibility–age model proposed by Kukla and An (1989) can also be questioned as there is no clear mechanism to support it. Misinterpretation of the expressions of the climatic cycles in the loess and an injudicious tuning procedure make a previously orbitally tuned time scale (Lu et al., 1996) unreliable. Recent studies show that there is a positive relationship between the dust accumulation rate and grain size distribution, allowing several age models to be developed for cal-

* Corresponding author. Fax: +86 29 552 2566; E-mail: luhy@loess.llqg.ac.cn

0031-0182/99/$ – see front matter
PII: S0031-0182(99)00113-3

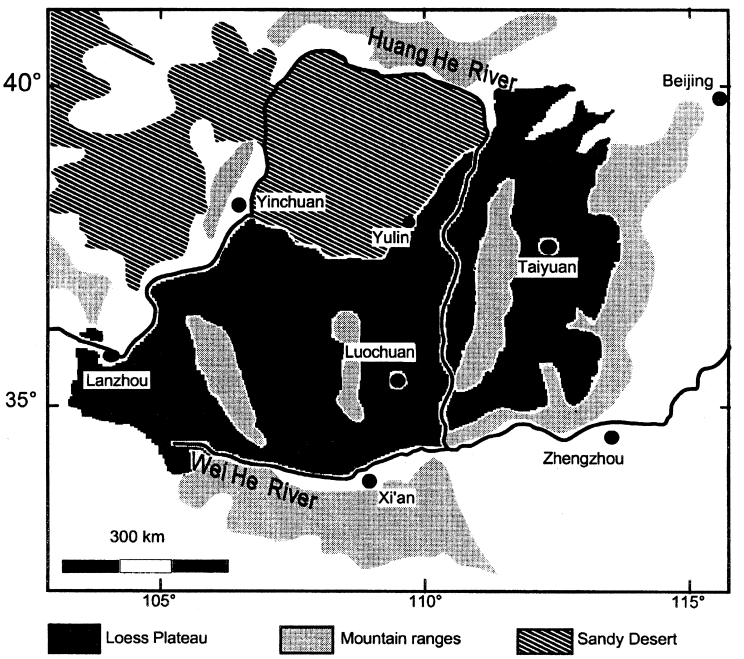

Fig. 1. The location of Luochuan on the Chinese Loess Plateau.

culating ages of loess–paleosol deposits (Porter and An, 1995; Vandenberghe et al., 1997). But further work is needed to seek the ideal proxy index of grain size because these results are still controversial. In short, it is necessary to build a more reliable time scale for the classic loess–paleosol sequence in central China for recognizing landscape response of the East Asian continental paleoclimate regime during the late Cenozoic.

The Milankovitch paleoclimatic theory has been widely accepted since the work of Hays et al. (1976). The Earth's orbital parameters change due to the gravitational forces between Earth and other celestial bodies and cause variability in solar insolation across the latitudes and seasons. It is believed that these changes triggered the late Cenozoic glacial–interglacial climatic oscillations which are recorded globally (Imbrie et al., 1984; Berger and Loutre, 1991; Shackleton et al., 1995).

Quantifying the main forcing mechanisms of the variability of the East Asian monsoon strength on time scales of 10^4 years remains a controversial topic. But it is widely accepted that there should be a relationship with solar radiation and Earth ice volume changes (e.g. An et al., 1990, 1991a; Ding et al., 1995; Liu and Ding, 1998). Previous spectral analyses of loess–paleosol paleoclimatic time series have shown that the main orbital cycles of 41, 23 and 19 kyr are recorded in the Chinese loess series (Kukla et al., 1990; Ding et al., 1994; Lu, 1996; Van Huissteden et al., 1997).

In this paper we compare paleoclimate variations recorded in the loess–paleosol sequence with the solar radiation variations calculated by Berger and Loutre (1991), and we develop an age model by tuning the magnetic susceptibility curves to the solar insolation variations. On the basis of this careful tuning, we aim to obtain a more reliable time scale than has hitherto been available for the loess–paleosol deposits of the central Chinese Loess Plateau.

2. Paleoclimatic proxy index variations and the tuning target curve

2.1. Paleoclimatic proxy index and the preliminary time scale

The magnetic susceptibility record in Chinese loess deposits has been shown to be an excellent

proxy index of East Asian summer monsoon intensity, although further work is needed to explain the details of the mechanism involved (An et al., 1990, 1991a; Zhou et al., 1990; Maher and Thompson, 1992). We therefore apply magnetic susceptibility as the paleoclimatic proxy index. The classic loess–paleosol profile at Luochuan (Fig. 1) was measured for field magnetic susceptibility in 1987 by Kukla and An (1989), and we systematically sampled this profile again in the summer of 1993. For the paleosol units, the sampling interval was 3 cm, and for the loess units the sampling interval was 5 cm. All the samples were measured for magnetic susceptibility using a Bartington Instruments MS-2 magnetic susceptibility meter at the State Key Laboratory of Loess and Quaternary Geology in Xi'an (Lu, 1996) (Fig. 2). A good correlation was found to be evident between our results and those of Kukla and An (1989).

At Luochuan, the Early Pleistocene loess–paleosol formation (Wucheng Formation) has been primarily divided into four loess–paleosol complexes through field observations and magnetic susceptibility measurements (Liu et al., 1985; Kukla and An, 1989). It is not easy to see in detail the loess and paleosol units by field observation at this location. However, we regard the time resolution and expression of the Wucheng Formation at Luochun as being as good as at other places, such as at Baoji in the southern part of the Loess Plateau (Ding et al., 1994), where clear loess–paleosol alternations can be identified in the field. The Baoji profile is therefore regarded as better than that at Luochuan for studying the paleoclimate of the Early Pleistocene on the Chinese Loess Plateau. We carefully compared our Luochuan magnetic susceptibility record with the grain size record of the Baoji profile for the Wucheng Formation. Main variations in the two proxy indices, which are strongly related to the paleoclimate variations, can be easily correlated (Fig. 3). This strong correlation can be supported because the loess and paleosol stratigraphies are quite stable and clearly recognisable over large areas of the Loess Plateau. The magnetic susceptibility record demonstrates that the Wucheng Formation at Luochuan is also a typical profile for loess deposits in central China.

Biostratigraphy and paleomagnetic stratigraphic research demonstrates that the onset of loess accumulation at Luochuan was either 2.35 Ma (Kukla and An, 1989) or around 2.5 Ma ago (Yue, 1995; Liu and Ding, 1998). Here we assume that the dust sedimentation rate in loess units was double that in the paleosol units (An et al., 1991a; Ding et al., 1994). We interpolate ages between the top (present, 0 kyr BP) and several magnetic reversals (the Brunhes/Matuyama polarity reversal boundary at 780 kyr BP; the Matuyama/ Olduvai polarity reversal boundary at 1757 kyr BP and the Matuyama/Gauss polarity reversal boundary at 2600 kyr BP) to obtain a preliminary time scale (Fig. 2). Spectral analysis techniques and band-pass filters centered on the frequencies of the orbital cycles have been applied on this preliminary time series. Results show that the obliquity (41 kyr) and precession

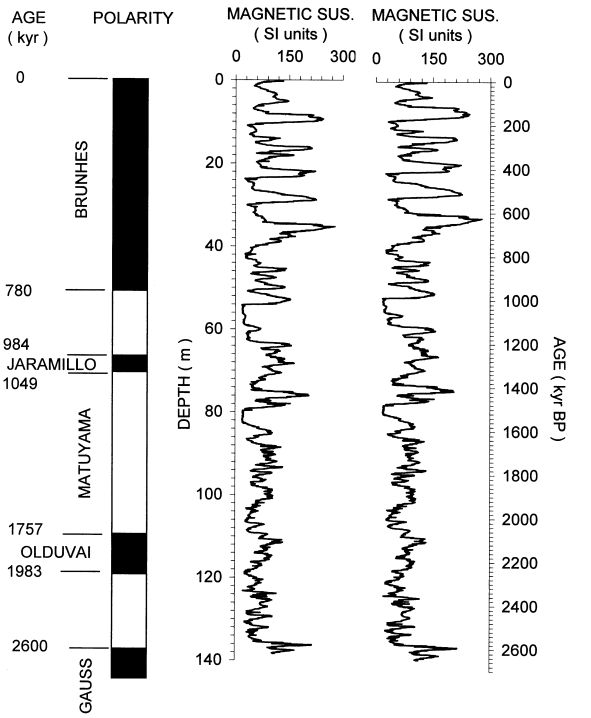

Fig. 2. Magnetic susceptibility variations of the Luochuan loess–paleosol sequence versus depth and versus a preliminary time scale. Positions of geomagnetic polarity reversal points were determined by Kukla and An (1989), and the preliminary time scale was obtained by interpolating ages along four age control points (top of the sequence, 0 kyr BP, B/M boundary at 780 kyr BP, M/O boundary at 1757 kyr BP and M/G boundary at 2600 kyr BP) and by assuming that the dust sedimentation rate in loess was double that of the paleosol.

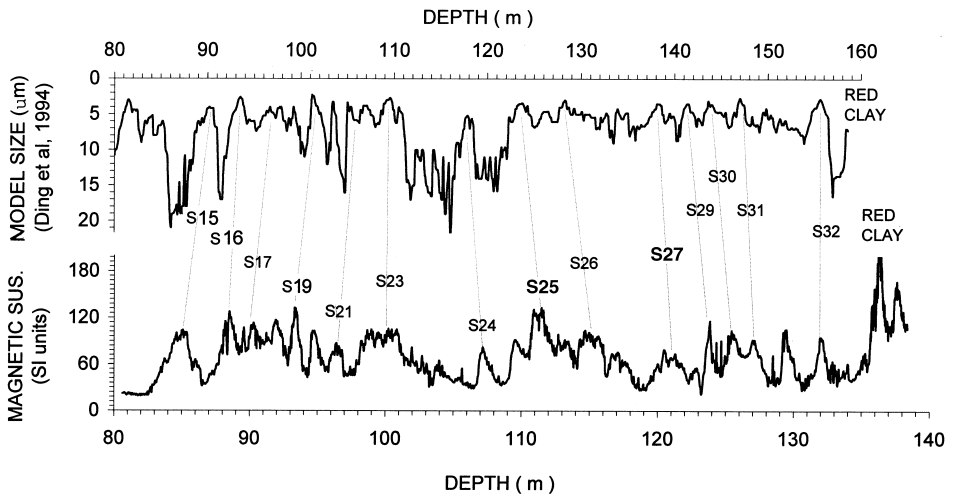

Fig. 3. Correlation between variations of magnetic susceptibility of the Wucheng loess–paleosol deposits at Luochuan and the modal grain size record for Boaji (Ding et al., 1994).

cycles (23 kyr and 19 kyr) are obtained from the preliminary magnetic susceptibility time series (Fig. 4), thus proving that the East Asia summer monsoon changes are linked to solar radiation variations from Milankovitch forcing on a 10^4 years time scale. There are some unreliable preliminary time scales or harmonics of the orbital cycles in the time series and these may cause the non-orbital frequencies seen by the spectral analysis (Fig. 4).

2.2. The target curve

There are many approaches for tuning sediment sequences to astronomical data, but there are a few substantial differences between them (Martinson et al., 1987). Since variations in the intensity of the East Asian summer monsoon correlate with solar insolation changes at the orbital time scale in the past, and since the boundary conditions of the Northern Hemisphere during the glacial–interglacial periods were strongly tied to latitude 65°N insolation, we chose the summer solar radiation values at 65°N for the past 2.7 million years as the target curve. Liu and Ding (1998) also used this target curve in tuning the time scale for other loess–paleosol deposits in the Loess Plateau. The solar radiation estimate latitude 65°N is also regarded as a typical indication for Northern Hemisphere radiation conditions (Imbrie et al., 1984;

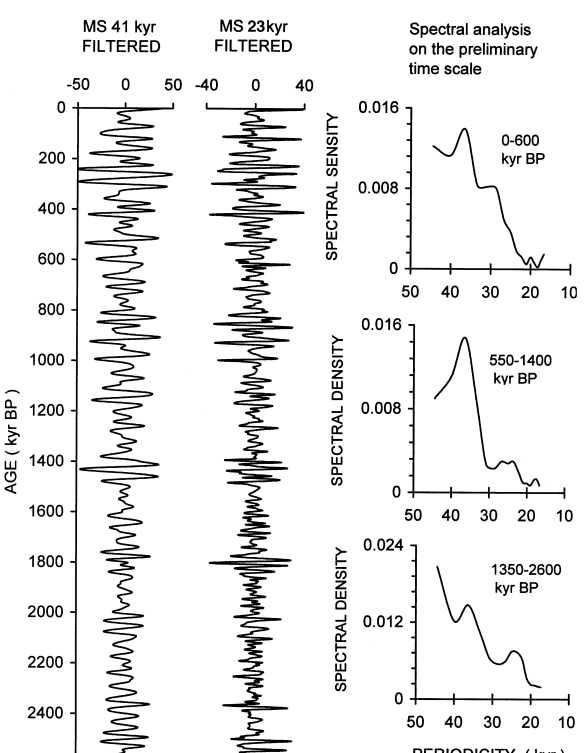

Fig. 4. Band-pass filtered results centered on 41 kyr and 23 kyr cycles and spectral analysis on the preliminary time scale. The results show that the 41 kyr and 23 kyr periodicities are presented through this preliminary time series.

Berger and Loutre, 1991). In this study the phase relationship between the magnetic susceptibility proxy index and the solar insolation changes was determined by comparing absolutely dated paleoclimatic records and orbitally induced insolation variations during the past 10,000 years. There are 5-kyr lags between solar insolation forcing and monsoon climate response in the Holocene (An et al., 1991a) so we assumed that this 5-kyr phase difference existed between the solar insolation curves and monsoon climate response throughout the last 2.7 Ma.

3. Orbital tuning

First, we adjusted the preliminary magnetic susceptibility time series with the 65ºN latitude summer solar insolation time series by adding age control points, to improve the match between the two time series. During the tuning process, we paid special attention to paleosol units as these have a lower time resolution than loess units. In the intervals of loess formation, dust accumulation rates were higher and it is easier to see the bands of solar radiation forcing (Liu et al., 1985; An et al., 1991b; Ding et al., 1994). Since the loess units offer a higher time resolution than paleosol units, some short climate cycles may not be as prominently recorded in the paleosol units at Luochuan. Notwithstanding this, short climatic cycles within paleosol units are often clearly evident in more northwesterly regions of the Loess Plateau. For instance, the paleosol deposit S1 of the last interglacial period (between 73 and 129 kyr BP) at Luochuan does not record the three precession-related oscillations clearly. But these three peaks can be clearly seen in the loess–paleosol deposit at Huanxian in the northwest of the Loess Plateau. Therefore, when tuning the time scale for the Luochuan sediments, we also refer to the paleoclimatic record from the northwest to assist in interpreting the short climatic variations.

The magnetic susceptibility and the 65ºN latitude summer solar insolation time series were visually matched. Then the magnetic susceptibility time series was filtered using a band-pass filter centered on the 41-kyr and 23-kyr frequencies, and the resulting curves were correlated with the unfiltered solar insolation time series. Additional age control points were added iteratively until the unfiltered magnetic susceptibility time series and solar radiation time series showed a good match, as confirmed by cross-spectral analyses (see below). We used a cubic spline interpolation technique on the additional age points to improve covariance of the magnetic susceptibility and insolation time series (Fig. 5). The results place the ages of the boundaries between the Malan and Lishi, and the Lishi and Wucheng loess formations at 71 and 1320 kyr BP, respectively, and the onset of loess accumulation at 2470 kyr BP.

4. Testing the new time scale

4.1. Comparison with the absolute geomagnetic polarity reversal ages

Accurate and reliable ages of geomagnetic polarity reversals were obtained on the basis of precise Ar/Ar radiometric dating on carefully selected single crystals of sanidine from lavas (Baksi, 1992; Singer, 1995). The new geomagnetic polarity time scale (GPTS) for the Cenozoic developed by Cande and Kent (1992) shows that the ages of the magnetic boundaries, which are older than those of previous GPTS (Bregen et al., 1985), are in accordance with the astronomically tuned time scale (Johnson, 1982; Shackleton et al., 1990; Bassinot et al., 1994). The positions of several geomagnetic reversal boundaries recorded in the Luochuan loess–paleosol sequence have been located by several investigators (Heller and Liu, 1982; Liu et al., 1985; Kukla and An, 1989; Yue, 1995). The ages of magnetic reversal boundaries from our astronomical calibration agree well with those obtained by absolute radiometric measurements (see Table 1). For the Brunhes/Matuyama (B/M) boundary there is a difference of 11 kyr, and for the boundaries of the Olduvai subchron and Matuyama reversed chron there are differences of 47, 32 and 30 kyr, respectively. The discrepancies in these magnetic reversal ages are less than 5% (Table 1).

4.2. Cross-spectral analysis

In order to test the coherency between our new magnetic susceptibility time series and the insola-

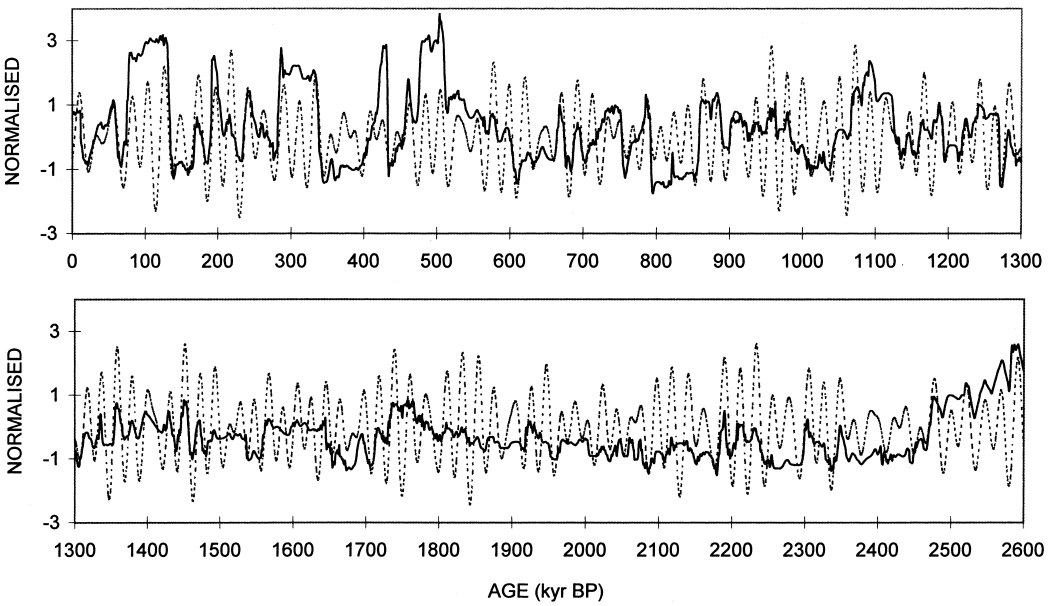

Fig. 5. Correlation between magnetic susceptibility variations plotted on the new time scale (solid line) and solar insolation variations for 65ºN (Berger and Loutre, 1991) (dashed line) for the past 2600 kyr.

tion time series, spectral analyses were conducted on both time series. Results indicate that on the orbital periodicities 41 kyr, 23 kyr and 19 kyr, the coherency is significant and is over the 95% significance level at 0.61 (Fig. 6). During the interval of 0–600 kyr BP, the coherency was high in the orbital frequency cycle, with values significantly within the 95% confidence interval limit, with a coherency measure of 0.915 for precession (23 kyr) (Fig. 6). Phase lags behind the orbital forcing over the frequency bands are 8.97 kyr, 5.28 kyr and 6.01 kyr for obliquity (41 kyr) and precession (23 kyr and 19 kyr), respectively (Table 2), being approximately consistent with the values estimated by Ding et al. (1994). During the 550–1400 kyr BP interval, the coherencies were also high in the orbital frequency cycles, with values within the 95% confidence interval limit, and with coherency measures of 0.892 and 0.879 for precession (19 kyr and 23 kyr), respectively (Fig. 6). Phase lags behind the orbital forcing over the frequency bands are 5.08 kyr, 5.09 kyr and 5.34 kyr for obliquity (41 kyr) and precession (23 kyr and 19 kyr), respectively. During the 1350–2600 kyr BP interval, the coherencies were also high in the orbital frequency cycles, with values falling within the 95% confidence interval limit, and with measure coherencies of 0.748, 0.881 and 0.852 for obliquity (41 kyr) and precession (19 kyr and 23 kyr), respectively (Fig. 6). Phase lags behind the orbital forcing over the frequency bands are 6.71 kyr, 5.07 kyr and 6.39

Table 1
Comparison of magnetic reversal ages obtained using our time scale with ages determined by Cande and Kent (1992)

Reversal points	B/M	M/J	J/M	M/O	O/M	M/G
Ages (kyr BP) (Cande and Kent, 1992)	780	984	1049	1757	1983	2600
This work (kyr BP)	769	946	1001	1710	1951	2630
Differences (%)	1.41	3.86	4.58	2.68	1.61	−1.15

B = Brunhes; M = Matuyama; J = Jaramillo; O = Olduvai.

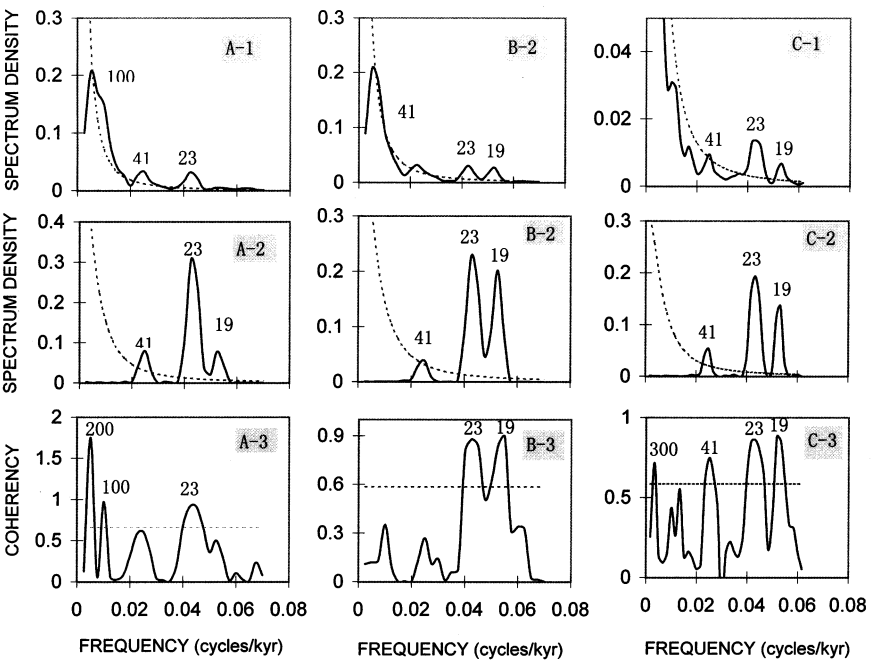

Fig. 6. The spectral and cross-spectral analysis results of the orbital tuned MS time series and solar insolation variations for the past 2600 kyr. The dashed line shows the significance level of $\alpha = 0.05$. *A* = 0–600 kyr BP: *A-1* = MS time series, *A-2* = solar radiation time series, *A-3* = cross-spectral analysis. *B* = 550–1400 kyr BP: *B-1* = MS time series, *B-2* = solar radiation time series, *B-3* = cross-spectral analysis. *C* = 1350–2600 kyr BP: *C-1* = MS time series, *C-2* = solar radiation time series, *C-3* = cross-spectral analysis.

Table 2
Phase lag times (kyr) of the loess susceptibility with reference to insolation cycles of periods of 41, 23 and 19 kyr

Periodicity (kyr)	Age (kyr)			
	0–600	550–1400	1350–2600	0–2600
41	8.97	5.08	6.71	7.3
23	5.28	5.09	5.07	5.21
19	6.01	5.34	6.39	5.83

kyr for obliquity (41 kyr) and precession (19 kyr and 23 kyr), respectively (Table 2). Phase lags estimates between the whole time series and the solar insolation time series is presented in Table 2. Coherency is also high for the non-orbital periodicities at 100 kyr, 200 kyr and 300 kyr. These may be explained by the climate system responding to factors other than insolation forcing. The mechanisms that drive these non-orbital scale cycles of the East Asia summer monsoon are not clear.

5. Discussion

There is controversy resulting from the previously developed time scales for loess–paleosol sequences in the Chinese Loess Plateau (Liu et al., 1985; Kukla et al., 1990; Ding et al., 1994; Vandenberghe et al., 1997). This results, for instance, in around 30 kyr age differences for the 'marker' S5 paleosol unit at Baoji and that at Luochuan. The results of Kukla et al. (1990) show that this strikingly marked layer formed around 480–605 kyr BP, while other workers place this unit between 482–579 kyr BP (Ding et al., 1994) and 450–600 kyr BP (Vandenberghe et al., 1997). These discrepancies may be caused by misinterpretation for the climatic cycles recorded by the loess–paleosol deposit in the orbital time scale (Ding et al., 1994), perhaps uncertainties in the origin of magnetic susceptibility (Kukla and An, 1989), or the effects of sediment compaction (Vandenberghe et al., 1997) on the actual sedimentation rate. Our new time scale for the typical loess deposits at Luochuan are close to the time scale of Ding et al. (1994) for the

loess–paleosol units above the S8 paleosol units at Baoji, but are different for the deposits below the S8 unit. We think that these differences may be caused by misinterpretations of the climatic cycles in the Wucheng loess–paleosol formation, which are difficult to see clearly, and differences in the climatic proxy indices used in the two studies. A ratio of coarse and fine grain size fractions was used as a proxy index of the monsoon changes by Ding et al. (1994). However the different climatic implications of the two grain size fractions means that a ratio proxy index may not correctly record climatic cycles, meaning that some climatic changes may be missed (Lu, 1996). Since we believe that the magnetic susceptibility is a good proxy of the monsoon strength on the 10^4 yr time scale, it should be useable for reconstructing the monsoonal system changes in the past. Vandenberghe et al. (1997) have developed an absolute time scale for the loess deposit at Luochuan, and this time scale can be partly correlated with our new time scale, but many discrepancies remain. We think that the statistical relationship between sedimentation rates and the grain size proxy index should be further examined. A better knowledge of compaction rates would also help to improve development of the time scale. Overall, we believe the present time scale is a good one if there are no substantial disconformities in the loess–paleosol sequences (Kukla and An, 1989).

Our new orbitally tuned age model presents a more detailed calibration for the East Asian monsoon climate history for the Quaternary. The onset of loess deposition in the central Chinese Loess Plateau is thus estimated at 2470 kyr BP, thus indicating a new threshold of both progressive aridity in the interior of China and the strength of the winter monsoon flow. This may have been caused by the expansion of the ice sheet in the Northern Hemisphere (Shackleton et al., 1995) or the accelerated uplift of the Tibet Plateau. Both these factors would cause a strengthening of the monsoon climate pattern (Lu, 1996; Ruddiman, 1997). Thus from this new time scale we propose that at around 2470 kyr BP the East Asian monsoon was significantly strengthened with the winter monsoon circulation distributing a mantle of loess in central China. The relatively warmer and wetter climate of the Pliocene was thus replaced by fluctuations of cold and dry climate with warmer and wetter climates (An et al., 1990; Liu and Ding, 1998). At around 1320 kyr BP a further threshold of the monsoon climate was crossed in central China. High-frequency and small-scale oscillations of the amplitude of the monsoon climate were replaced by lower-frequency and large-amplitude oscillations. Also we note that the monsoon climate has been dominated by large-scale amplitude oscillations in the 100,000 year band over the last 580 kyr BP. These two scale shifts may have been caused by an accelerated uplift of the Tibet Plateau; elsewhere simulations have shown that the monsoon system can be strengthened as the altitude of the Tibet Plateau increases (Ruddiman, 1997). The Northern Hemisphere ice volume could not be a main factor in driving these climate shifts because it was stationary at the key threshold times.

There are several climatic extremes (Guo et al., 1998) recorded by magnetic susceptibility from the Loess Plateau. The easily identified L9 and L15 loess units, which may indicate two exceptionally dry and cold climate periods, have particularly high sedimentation rates. By our new age model, the L9 and L15 units represent 65 kyr and 71 kyr of accumulation, respectively, and these estimates are different from those obtained by sedimentation rate calculations (Liu et al., 1985; Vandenberghe et al., 1997). Careful analysis of the magnetic susceptibility in L9 and L15 indicate variations of the signal values. The variations could be driven by solar radiation over such time frames and three precession-related climatic cycles may therefore be recorded for these periods. Two relatively warmer and wetter climates are seen for S5 and S13. These two climate patterns have estimated ages of 472–576 kyr BP and 1061–1120 kyr BP. We have not recognised parallels for these climatic extremes in the deep-sea $\delta^{18}0$ records (Shackleton et al., 1990). Thus these climatic periods may not be explained by ice volume forcing. If the East Asian monsoon climate and the Northern Hemisphere ice volume were de-coupled in these intervals it may be evidence that the monsoon climate system was not always driven by the ice volume and solar radiation variations.

6. Summary

The magnetic susceptibility of the loess–paleosol sequences of the central Chinese Loess Plateau is

a good proxy index of East Asia summer monsoon variations (An et al., 1990, 1991a). Thus, a detailed measurement in magnetic susceptibility of the loess–paleosol deposits can give information on the East Asia summer monsoon changes in the past. Because the East Asia summer monsoon variations over the Quaternary period can at least partly be accounted for by the solar insolation forcing on a 10^4 yr time scale, we developed an age model by tuning the magnetic susceptibility series to the summer solar insolation changes at 65°N latitude. In this age model, the ages of the boundaries between the Malan and Lishi, and Lishi and Wucheng loess formations are 71 and 1320 kyr BP, respectively. The onset of loess accumulation is at 2470 kyr BP (Table 3), and several climatic extremes in that of L9 and L15 loess units and that of S5 and S13 paleosol units over the Loess Plateau were calibrated. The new age model was tested by comparing the orbital derived ages with absolute age determination of magnetic reversals, and by spectral and cross-spectrum analyzing. These indicate that the calibration provides a reliable time scale for the Luochuan loess–paleosol deposit.

Table 3
Ages of paleosol layers of the Luochuan loess profile

Paleosol units	Age of top (kyr BP)	Age of bottom (kyr BP)
S1	71	129
S2	188	254
S3	279	334
S4	385	428
S5	471	576
S6	658	670
S7	706	748
S8	760	788
S9	853	883
S10	895	916
S11	946	957
S12	967	1000
S13	1061	1120
S14	1214	1265
S15	1273	1295
S16	1327	1360
S17	1386	1404
S18	1421	1429
S19	1440	1451
S21	1488	1531
S23	1592	1640
S24	1682	1696
S25	1727	1800
S26	1913	1945
S27	2105	2143
S29	2178	2189
S30	2200	2212
S32	2337	2359

Acknowledgements

We thank two anonymous reviewers for significantly improving an early version of this manuscript and Mr. Wenfeng Yang for much help. Prof. Vandenberghe and Mr. Nugteren participated in the fieldwork. This work was partly supported by the 9.5 key research project fund of the Chinese Academy of Sciences (KZ951-A1-402), and the 973 Tibet Programme of the State Science and Technology Commission of China (SSTC).

References

An, Z.S., Liu, T.S., Lou, Y.C., Porter, S.C., Kukla, G., Wu, X.H., Hua, Y.M., 1990. The long-term palaeomonsoon variation recorded by the loess–paleosol sequence in central China. Quat. Int. 7/8, 91–95.

An, Z.S., Kukla, G., Porter, S.C., Xiao, J.L., 1991a. Magnetic susceptibility evidence of monsoon variation on the Loess Plateau of central China during the last 130000 years. Quat. Res. 36, 29–36.

An, Z.S., Kukla, G., Porter, S.C., Xiao, J.L., 1991b. Late Quaternary dust flow on Chinese Loess Plateau. Catena 18 (2), 125–132.

Baksi, A., 1992. $^{40}Ar/^{39}Ar$ dating of the Brunhes–Matuyama geomagnetic field reversal. Science 256, 356–357.

Bassinot, F.C., Labeyrie, L.D., Vicent, E., Quidelleur, X., Shackleton, N.J., Lancelot, Y., 1994. The astronomical theory of climate and the age of the Brunhes–Matuyama magnetic reversal. Earth Planet. Sci. Lett. 126, 91–108.

Berger, A., Loutre, M.F., 1991. Insolation values for the climate of the last 10 million years. Quat. Sci. Rev. 10, 297–317.

Berggren, W.A., Kent, D.V., Van Couvering, J.A., 1985. The Neogene, Part 2. Neogene geochronology and chronostratigraphy. In: Snelling, N. (Ed.), The Chronology of Geological Record. Mem. Geol. Soc. London 10, 211–260.

Cande, S.C., Kent, D.V., 1992. A new geomagnetic polarity time scale for the late Cretaceous and Cenozoic. J. Geophys. Res. 97, 13917–13951.

Ding, Z.L., Yu, Z.W., Rutter, N.W., Liu, T.S., 1994. Towards an orbital time scale for Chinese loess deposit. Quat. Sci. Rev. 13, 39–70.

Ding, Z.L., Yu, Z.W., Liu, T.S., 1995. Ice-volume forcing of East

Asian winter monsoon variations in the past 800,000 years. Quat. Res. 44, 149–159.

Guo, Z.T., Liu, T.S., Fedroff, N., Wei, L.Y., Ding, Z.L., Wu, N.Q., Lu, H.Y., Jiang, W.Y., An, Z.S., 1998. Climate extremes in loess of China coupled with the strength of deep water formation in the North Atlantic. Global Planet. Change 18, 113–128.

Hays, J.D., Imbrie, J., Shackleton, N.J., 1976. Variation in the Earth's orbit: pacemaker of the ice ages. Science 194, 1121–1132.

Heller, F., Liu, T.S., 1982. Magnetostratigraphical dating of loess deposits in China. Nature 300, 431–432.

Imbrie, J., Hays, J.D., Martinson, D.G. et al., 1984. The orbital theory of Pleistocene climate: support from a revised chronology of the marine $\delta^{18}O$ record. In: Berger, A., Imbrie, J., Hays, J., Kukla, G., Saltsman, B.G. (Eds.), Milankovitch and Climate, Part 1. Reidel, Dordrecht, pp. 269–305.

Johnson, R.G., 1982. Brunhes–Matuyama magnetic reversal dated at 790,000 yr B.P. by marine–astronomical correlations. Quat. Res. 17, 135–147.

Kukla, G., An, Z.S., 1989. Loess stratigraphy in central China. Palaeogeogr., Palaeoclimatol., Palaeoecol. 72, 203–223.

Kukla, G., An, Z.S., Meliece, L., Gavin, G., Xiao, J.L., 1990. Magnetic susceptibility record of Chinese loess. Trans. R. Soc. Edinburgh: Earth Sci. 81, 263–288.

Liu, T.S., Ding, Z.L., 1998. Chinese loess and the paleomonsoon. Annu. Rev. Earth Planet. Sci. 26, 111–145.

Liu, T.S., et al. 1985. Loess and Environment. China Ocean Press, Beijing, pp. 31–67.

Lu, H.Y., 1996. East Asian Palaeomonsoonal Climate Variation During the Last 2.5 Myr Recorded by Chinese Loess Deposits. Unpublished PhD Thesis, Nanjing University, Nanjing.

Lu, H.Y., An, Z.S., Yang, W.F., 1996. A preliminary time scale for loess stratigraphy at Luochuan, central China. Geol. J. Univ. 2, 230–236.

Maher, B.A., Thompson, R., 1992. Palaeoclimatic significance of the magnetic record of the Chinese loess and paleosols. Quat. Res. 37, 155–170.

Martinson, D.G., Pisias, N.G., Hays, J.D., Imbrie, J., Moore, T.C., Shackleton, N.J., 1987. Age dating and the orbital theory of the ice ages: development of a high-resolution 0 to 300,000-year chronostratigraphy. Quat. Res. 27, 1–29.

Porter, S.C., An, Z.S., 1995. Correlation between climate events in the North Atlantic and China during the last glaciation. Nature 375, 305–308.

Ruddiman, W.F., 1997. Tectonic Uplift and Climate Change. Plenum Press, New York, 511 pp.

Shackleton, N.J., Berger, A., Peltier, W.R., 1990. An alternative astronomical calibration of the lower Pleistocene timescales based on ODP site 677. Trans. R. Soc. Edinburgh: Earth Sci. 81, 251–261.

Shackleton, N.J., Hall, M.A., Pate, D., 1995. Pliocene stable isotope stratigraphy of site 846. Proc. ODP Sci. Results 138, 337–355.

Singer, B.S., 1995. The age and duration of the Matuyama–Brunhes geomagnetic reversal from $^{40}Ar/^{39}Ar$ incremental heating analysis on Chilean and Tahitian lavas. Terra Nova, Abstr. Suppl. 1 (7), 349.

Vandenberghe, J., An, Z.S., Nugteren, G., Lu, H.Y., Huissteden, K.V., 1997. New absolute time scale for the Quaternary climate in the Chinese loess region by grain-size analysis. Geology 25, 35–38.

Van Huissteden, J., Nugteren, G., Vandenberghe, J., An, Z.S., 1997. Spectral analysis of a grain size record of the loess deposits in Central China. Proc. 30th Int. Geol. Congr., Vols. 2, 3, VSP, pp. 313–325.

Yue, L.P., 1995. Magnetic reversal and their geological significance recorded by loess and red clay deposit in China. Acta Geogr. Sin. 38 (3), 311–319.

Zhou, L.P., Oldfield, F., Wintle, A.G., Robinson, S.G., Wang, J.T., 1990. Partly pedogenic origin of magnetic variations in Chinese loess. Nature 346, 77–739.